**Office Note Series on
Global Modeling and Data Assimilation**

Siegfried Schubert, Editor

Documentation of the Physical-Space Statistical Analysis System (PSAS) Part II: The Factored-Operator Formulation of Error Covariances

J. Guo[†]
J. W. Larson[*]
G. Gaspari[†]
A. da Silva
P. M. Lyster[*]

Data Assimilation Office, Goddard Laboratory for Atmospheres
[†] *General Sciences Corporation, Laurel, Maryland*
[*] *Earth System Science Interdisciplinary Center (ESSIC), University of Maryland*

Robert M. Atlas, Acting Head
Data Assimilation Office
Goddard Space Flight Center
Greenbelt, Maryland 20771

Revision History

This Office-Note 98-04 was first produced for the PSAS Software Workshop on October 26, 1998.

Version Number	Version Date	Pages Affected/ Extent of Changes	Aproval Authority
Version 1β	October 26, 1998	First draft (before review) from PSAS Workshop	
Version 1	December 6, 1999	Initial release	ON Editor

Abstract

This article is a theoretical basis for the software implementation of the Physical-space Statistical Analysis System (PSAS) that is used for atmospheric data analysis at the NASA Data Assimilation Office (DAO). The PSAS implements a statistical algorithm that combines irregularly spaced observations with a gridded forecast to produce an optimal estimate of the state of the atmosphere. Starting from models for the forecast and observation errors, the PSAS (version v1.5.1) uses a factored-operator formulation for the error covariance matrices. This formulation determines how the observational data, and their attributes, as well as the error covariance matrices are managed during the life cycle of the algorithm: this is the main source of *software complexity* of the PSAS. This is mainly due to the diversity of data types and sources, as well as the use of the multivariate formulation as described in the text. The coordinate systems and data types used in the PSAS analysis are described. The PSAS univariate forecast error covariance models are introduced, and the multivariate upper-air and sea-level coupled height-wind and decoupled wind forecast error covariance models are derived from the univariate height forecast error covariance models. The factorization of these multivariate covariance models into a product of matrices is described. Observation error covariances used in the PSAS are briefly discussed. Finally, we discuss the structure of the matrices in the software implementation of the PSAS and some related software issues.

An on-line version of this document can be obtained from

`ftp://dao.gsfc.nasa.gov/pub/office_notes/on199804v1.1.ps.Z (postscript)`

Visit also the Data Assimilation Office's Home Page at

`http://dao.gsfc.nasa.gov/`

Contents

List of Figures

List of Tables

1   Preface

The purpose of this article is to describe, at a symbolic level, the software representation of error covariance matrices used in the Physical-space Statistical Analysis System (PSAS). The articles describing the PSAS are as follows:

1. da Silva, A., and J. Guo, 1996: Documentation of the Physical-Space Statistical Analysis System (PSAS) Part I: The Conjugate Gradient Solver Version, PSAS-1.00. *DAO Office Note 96-02*.

2. Guo J., J. W. Larson, G. Gaspari, A. da Silva, and P. M. Lyster, 1998: Documentation of the Physical-Space Statistical Analysis System (PSAS) Part II: The Factored-Operator Formulation of Error Covariances. *DAO Office Note 98-04*.

3. Larson J. W., J. Guo, G. Gaspari, A. da Silva, and P. M. Lyster, 1998: Documentation of the Physical-Space Statistical Analysis System (PSAS) Part III: The Software Implementation of the PSAS. *DAO Office Note 98-05*.

4. da Silva A., M. Tippett, and J. Guo, 1999: The PSAS User's Manual. To be published as *DAO Office Note 99-XX*.

2   Introduction

Operational data assimilation systems and numerical weather prediction centers have recently replaced older optimal interpolation (OI) systems that localize the analysis problem, by so-called *global* analysis systems that use all observations available at a given synoptic time. The change to global analysis systems was driven partly by the need to improve analyses by eliminating the effects of *local approximation* and *data selection* inherent in OI systems (Cohn *et al.* 1998).

Global statistical analysis systems now in place at the U.S. National Centers for Environmental Prediction (NCEP; Parrish and Derber 1992), and at the European Centre for Medium-Range Weather Forecasts (ECMWF; Courtier *et al.* 1998, Rabier *et al.* 1998, Andersson *et al.* 1998) are *variational* analysis schemes formulated directly in spectral (spherical harmonic) space, rather than in physical space like OI schemes. The Physical-space Statistical Analysis System (PSAS) developed at the Data Assimilation Office (DAO) is a global statistical analysis system formulated directly in physical space. The design objectives of the PSAS, and the relationship between the PSAS, OI, and the aforementioned spectral variational schemes are summarized in DAO (1996, Secs. 5.2.1 and 5.2.2, cf. Cohn *et al.* 1998).

For computational efficiency, spectral analysis systems rely explicitly on the assumption that covariance matrices are diagonal in spherical harmonic space, i.e., are obtained from correlation functions that are *isotropic* in physical space (Cohn *et al.* 1998, Sec. 5.1.1, cf. Gaspari and Cohn 1999, Theorem 2.11). Since the PSAS models error covariances directly in physical space, flow-dependent, anisotropic covariance functions can be incorporated into the statistical analysis. The ability to incorporate such covariances into the PSAS should result in improvements to the analyses (Cohn *et al.* 1998). In addition, compactly supported covariance functions can be incorporated in physical space (Gaspari and Cohn 1999). The PSAS exploits this fact to induce sparsity in covariance matrices, thereby reducing computational complexity in the statistical analysis.

The potential to improve analyses in the PSAS through better covariance modeling is a factor motivating many recent research efforts and much of the operational development at the DAO. One important goal of this article and of Larson *et al.* (1998) is to provide an interface between covariance modeling theory developed for the PSAS, and its practical implementation in the PSAS software.

Covariance models arise in the PSAS in the following statistical analysis equations:

The innovation equation:
$$(HP^fH^T + R)\mathbf{x} = \mathbf{w^o} - H\mathbf{w^f}; \tag{1}$$

and

The analysis equation:
$$\mathbf{w^a} - \mathbf{w^f} = P^fH^T\mathbf{x}, \tag{2}$$

where P^f is an $n \times n$ forecast error covariance matrix, R is a $p \times p$ observation error covariance matrix, H is a $p \times n$ matrix that maps gridded forecast vectors to observations on an unstructured grid, $\mathbf{w^o}$ is a $p-$vector of observations, $\mathbf{w^f}$ is an $n-$vector of the gridded forecast, and $\mathbf{w^a}$ is an analysis $n-$vector. The right hand side of Eqn. (1) is called the innovation vector or the *observed-minus-forecast* (OMF) residual, and the left hand side of Eqn. (2) is called the *analysis increment* (AI). Equation (1) is solved using a pre-conditioned conjugate gradient (CG) algorithm (Golub and van Loan 1989, cf. da Silva and Guo 1996). With the current system ($n = 10^6$ and $p = 10^5$ are the approximate values) setting up and solving Eqn. (1) costs about half the computational effort in the PSAS. The remaining effort is taken by the transformation in Eqn. (2) of $\mathbf{x}$ from observation to state space (Cohn

et al. 1998). A discussion of the *computational complexity* of the PSAS and the end-to-end Goddard Earth Observing System Data Assimilation System (GEOS DAS) is given in Lyster (1999).

This article is a theoretical basis for the software implementation of the PSAS that is used for atmospheric data analysis at the DAO. Starting from models for the forecast and observation errors (e.g., see Eqs. (35) and (36)), the PSAS (version v1.5.1) uses a factored-operator formulation for the error covariance matrices. This formulation determines how the observational data, and their attributes, as well as the error covariance matrices are managed during the life cycle of the algorithm: this is the main source of *software complexity* of the PSAS. This is mainly due to the diversity of data types and sources, as well as the use of the multivariate formulation as described in the text. This article explains the algorithm at a symbolic level. More specific details of the software implementation of the PSAS are described in Larson *et al.* (1998).

Suppose that C is a matrix extracted from the left-hand-side of Eqn. (1)– typical values of C are P^f, $HP^fH^T + R$, P^fH^T, or R. In traditional OI systems such as GEOS-1 DAS (Pfaendtner *et al.* 1995), C is explicitly formed elementwise as a matrix and the OI analysis equations solved directly. In the PSAS, C is represented implicitly, using only the information necessary to effect the transformation from a vector $\mathbf{z}$ to $C\mathbf{z}$. For instance, at the highest level, the factored operator formulation is used to transform the n-vector $\mathbf{x}$ to $(HP^fH^T + R)\mathbf{x}$ (Eqn. 1), and to evaluate $P^fH^T\mathbf{x}$ in the analysis equation (2).

The factored operator formulation has a number of desirable features that include:

- Because the factored-operator formulation is derived directly from the multivariate error models, it is extensible to observations such as wind speed or satellite radiance.

- Fewer floating point operations are required to transform $\mathbf{z}$ to $C\mathbf{z}$ when C is implicitly represented as a factored operator instead of explicitly represented as a matrix. See Appendix A for an example.

- Factoring an operator into a product of simpler operators aids the development of modular software.

This article is organized as follows. Section 3 defines the data types used in the analysis, and establishes the coordinate system and notation used throughout the article. In Section 4, the PSAS univariate forecast error covariance models are introduced. The multivariate upper air coupled height-wind and decoupled wind forecast error covariance models are derived from the univariate height forecast error covariance model. These multivariate covariance models are then expressed in the so-called factored operator formulation. Observation error covariances are discussed in Section 5. Section 6 discusses the structure of the matrices in the software implementation of the PSAS.

3   The PSAS Analysis

The PSAS v1.5.1 solves the statistical analysis equations for the same data types used in GEOS-1 DAS (Pfaendtner *et al.* 1995). For reference, these are:

- The univariate upper air water vapor mixing ratio (q) analysis.

- The multivariate sea level pressure (p_{sl}) and near surface winds (u_{sl}, v_{sl}) analysis.

- The multivariate upper air geopotential height (h) and winds (u, v) analysis.

The univariate moisture forecast error covariance model is discussed in Sec. 4.1. The multivariate upper-air and sea-level forecast error covariance models are discussed in Secs. 4.2 and 4.3 of this paper.

3.1 Forecast and Observational Data Attributes

The PSAS takes as input *observed-minus-forecast* (OMF) residuals $\mathbf{w^o} - H\mathbf{w^f}$ on an unstructured grid of observations (see Eqn. (1)), and produces *analysis increments* (AI) $(\mathbf{w^a} - \mathbf{w^f})$ as output on a regular grid (see Eqn. (2)). The input OMF are accompanied by the following *attributes*:

- The data type `kt`: currently from the list given above.
- The instrument class `kx`; e.g., rawinsonde, TOVS, and cloud-track winds – see da Silva and Redder (1995) and Larson *et al.* (1998) for a complete list.
- The latitude φ.
- The longitude λ.
- The pressure level in hPa.
- The sounding index `ks`.

This determines the location of distinct OMF's in three-dimensional space.

3.2 Coordinates Used in the PSAS

Spatial locations are given in pressure coordinates (λ, φ, p). The angles λ and φ are shown in Figure 1, and p is pressure. The covariance functions we define below are functions of two points $(\lambda_i, \varphi_i, p_i)$ and $(\lambda_j, \varphi_j, p_j)$. We often abbreviate these two points by i and j respectively. The rest of this section establishes further basic notation used in the paper.

The unit vectors in the directions of r, λ, and φ are denoted by $\hat{\mathbf{e}}_r$, $\hat{\mathbf{e}}_l$, and $\hat{\mathbf{e}}_m$, respectively. Note that our notation for the unit vectors $\hat{\mathbf{e}}_l$ and $\hat{\mathbf{e}}_m$ differs slightly from that typically used in standard textbooks (cf. Arfken 1970, p. 81). Our notation emphasizes that $\hat{\mathbf{e}}_l$ is a unit vector in the *longitudinal* direction and that $\hat{\mathbf{e}}_m$ is a unit vector in the *meridional* direction.

The vectors in $(\hat{\mathbf{e}}_r, \hat{\mathbf{e}}_l, \hat{\mathbf{e}}_m)$ form a right-handed triple, since

$$\hat{\mathbf{e}}_r \times \hat{\mathbf{e}}_l = \hat{\mathbf{e}}_m \tag{3}$$

$$\hat{\mathbf{e}}_l \times \hat{\mathbf{e}}_m = \hat{\mathbf{e}}_r, \tag{4}$$

$$\hat{\mathbf{e}}_m \times \hat{\mathbf{e}}_r = \hat{\mathbf{e}}_l. \tag{5}$$

The relation between the standard basis vectors $\hat{\mathbf{i}}$, $\hat{\mathbf{j}}$, and $\hat{\mathbf{k}}$ in Euclidean three-space, and $\hat{\mathbf{e}}_r$, $\hat{\mathbf{e}}_m$, and $\hat{\mathbf{e}}_l$ is given by:

$$\hat{\mathbf{e}}_r = \cos\lambda\cos\varphi\hat{\mathbf{i}} + \sin\lambda\cos\varphi\hat{\mathbf{j}} + \sin\varphi\hat{\mathbf{k}} \tag{6}$$

$$\hat{\mathbf{e}}_m = -\cos\lambda\sin\varphi\hat{\mathbf{i}} - \sin\lambda\sin\varphi\hat{\mathbf{j}} + \cos\varphi\hat{\mathbf{k}} \tag{7}$$

Figure 1: The spherical coordinate system used in PSAS.

$$\hat{\mathbf{e}}_l = -\sin\lambda\hat{\mathbf{i}} + \cos\lambda\hat{\mathbf{j}}. \tag{8}$$

We define the following differential operators:

$$\partial_l := \frac{1}{\cos\varphi}\frac{\partial}{\partial\lambda} \tag{9}$$

and

$$\partial_m := \frac{\partial}{\partial\varphi}. \tag{10}$$

These operators rotate the radial unit vector $\hat{\mathbf{e}}_r$ into the other unit vectors $\hat{\mathbf{e}}_l$ and $\hat{\mathbf{e}}_m$:

$$\partial_l\,\hat{\mathbf{e}}_r = \hat{\mathbf{e}}_l \tag{11}$$
$$\partial_m\,\hat{\mathbf{e}}_r = \hat{\mathbf{e}}_m. \tag{12}$$

Given the right-hand triples $(\hat{\mathbf{e}}_{r_i}, \hat{\mathbf{e}}_{l_i}, \hat{\mathbf{e}}_{m_i})$ and $(\hat{\mathbf{e}}_{r_j}, \hat{\mathbf{e}}_{l_j}, \hat{\mathbf{e}}_{m_j})$ at points i and j respectively,

we define the *polarity index* between $\hat{\mathbf{e}}_{x_i}$ and $\hat{\mathbf{e}}_{y_j}$ as the dot product

$$\tau_{ij}^{xy} := \hat{\mathbf{e}}_{x_i} \cdot \hat{\mathbf{e}}_{\mathbf{y_j}}, \tag{13}$$

where x and y belong to the set $\{r, l, m\}$. Since $\hat{\mathbf{e}}_r$, $\hat{\mathbf{e}}_l$, and $\hat{\mathbf{e}}_m$ are mutually orthogonal, we have that

$$\tau_{kk}^{xy} = \delta_{xy}, \quad k = i, j, \quad x, y \in \{r, l, m\} \tag{14}$$

where δ_{xy} is the Kronecker delta.

Abbreviate the polarity index between $\hat{\mathbf{e}}_{r_i}$ and $\hat{\mathbf{e}}_{r_j}$ by

$$\tau_{ij} := \tau_{ij}^{rr} := \hat{\mathbf{e}}_{r_i} \cdot \hat{\mathbf{e}}_{\mathbf{r_j}}. \tag{15}$$

Observe that τ_{ij} is the cosine of the angle between $\hat{\mathbf{e}}_{r_i}$ and $\hat{\mathbf{e}}_{r_j}$, i.e., the great circle distance on the unit sphere. We use the polarity index to parameterize correlations in what follows (cf. Gaspari and Cohn 1999, Sec. 2.b). The following relations hold:

$$\tau_{ij}^{mr} := \hat{\mathbf{e}}_{m_i} \cdot \hat{\mathbf{e}}_{\mathbf{r_j}} = \partial_{m_i} \tau_{ij} \tag{16}$$

$$\tau_{ij}^{lr} := \hat{\mathbf{e}}_{l_i} \cdot \hat{\mathbf{e}}_{\mathbf{r_j}} = \partial_{l_i} \tau_{ij} \tag{17}$$

$$\tau_{ij}^{rm} := \hat{\mathbf{e}}_{r_i} \cdot \hat{\mathbf{e}}_{\mathbf{m_j}} = \partial_{m_j} \tau_{ij} \tag{18}$$

$$\tau_{ij}^{rl} := \hat{\mathbf{e}}_{r_i} \cdot \hat{\mathbf{e}}_{\mathbf{l_j}} = \partial_{l_j} \tau_{ij} \tag{19}$$

$$\tau_{ij}^{mm} := \hat{\mathbf{e}}_{m_i} \cdot \hat{\mathbf{e}}_{m_j} = \partial_{m_j}\partial_{m_i} \tau_{ij} \tag{20}$$

$$\tau_{ij}^{ml} := \hat{\mathbf{e}}_{m_i} \cdot \hat{\mathbf{e}}_{l_j} = \partial_{l_j}\partial_{m_i} \tau_{ij} \tag{21}$$

$$\tau_{ij}^{lm} := \hat{\mathbf{e}}_{l_i} \cdot \hat{\mathbf{e}}_{m_j} = \partial_{m_j}\partial_{l_i} \tau_{ij} \tag{22}$$

$$\tau_{ij}^{ll} := \hat{\mathbf{e}}_{l_i} \cdot \hat{\mathbf{e}}_{l_j} = \partial_{l_j}\partial_{l_i} \tau_{ij}. \tag{23}$$

4 Forecast Error Covariance Models

The terms in Eqs. (1) and (2) that involve the forecast error covariance matrices (e.g., P^f, HP^fH^T, or P^fH^T) are *modeled* as functions of the locations i and j. The covariance functions that are used in the PSAS v1.5.1 restrict the horizontal dependence to τ_{ij}, i.e., they are based on the assumption of isotropy at each pressure level (see Gaspari and Cohn 1999). For example, the general multi-level, univariate forecast error covariance function for the variable type z is $P^z(\tau_{ij}, p_i, p_j)$, which we often abbreviate as $P_{ij}{}^z$. The matrices used in the PSAS are grid evaluations of the covariance functions. For instance, in the case of point observations such as rawinsondes (cf. Sec. 5 below), the matrix HP^fH^T is formed by evaluating the forecast error covariance function on the Cartesian product of the observation locations. Similarly, P^fH^T is formed by evaluating the forecast error covariance function on the Cartesian product of the analysis and observation locations. Section 6 provides a pedagogical example of how such a matrix may be formed. As stated in Section 2, the implementation of the PSAS does not form a stand-alone matrix, and details of this are presented in Larson *et al.* (1998).

4.1   Univariate Forecast Error Covariances

A general multi-level, univariate forecast error covariance function is defined by

$$P_{ij}^z := < z_i z_j >,\tag{24}$$

where $<>$ represents expectation, and z_k is the scalar error field at location $k = i, j$. In the PSAS (DAO 1996), this covariance function is modeled as:

$$P_{ij}^z = \sigma_i{}^z \rho_{ij}^z \sigma_j{}^z,\tag{25}$$

where $\sigma_k{}^z$ (i.e., $\sigma^z(\lambda_k, \varphi_k, p_k)$) is the forecast error standard deviation in variable z at $k = i, j$, and ρ_{ij}^z (i.e., $\rho^z(\tau_{ij}, p_i, p_j)$) is the correlation function. In this expression, and for rest of the paper, we usually do not show the arguments of the functions for notational convenience. In the PSAS, Eq. (25) pertains to the case where z is mixing ratio q, height h, or sea-level pressure p_{sl}. The analysis of mixing ratio observations is univariate, but the height and sea-level pressure observations are treated with associated winds in a multivariate analysis, whose forecast error covariance formulation we now describe.

4.2   Multivariate Upper-air Forecast Error Covariances

The multivariate upper air analysis uses height (h) and horizontal wind (u, v) observations. We review the following derivation of modeled coupled height-wind error and decoupled wind errors to illustrate the ensuing discussion – see also DAO (1996, Sec. 5.2.7).

The upper-air (ua) forecast error covariance function is defined as a 3×3 matrix:

$$P_{ij}^{ua} := < \vec{\epsilon}_i{}^{ua} \vec{\epsilon}_j{}^{ua T} >,\tag{26}$$

where $\vec{\epsilon}_k{}^{ua}$ ($k = i, j$) is the upper-air forecast error field. The error field is comprised of three terms

$$\vec{\epsilon}_k{}^{ua} := \vec{\epsilon}_k{}^h + \vec{\epsilon}_k{}^\psi + \vec{\epsilon}_k{}^\chi, \quad k = i, j,\tag{27}$$

where

$$\vec{\epsilon}_k{}^h := \begin{bmatrix} h_k \\ u_k^h \\ v_k^h \end{bmatrix}, \quad k = i, j,\tag{28}$$

is a vector of height forecast error (h_k) and height-coupled wind errors (u_k^h, v_k^h),

$$\vec{\epsilon}_k{}^\psi \equiv \begin{bmatrix} 0 \\ u_k^\psi \\ v_k^\psi \end{bmatrix}, \quad k = i, j,\tag{29}$$

and

$$\vec{\epsilon}_k{}^\chi \equiv \begin{bmatrix} 0 \\ u_k^\chi \\ v_k^\chi \end{bmatrix}, \quad k = i, j,\tag{30}$$

are height-decoupled wind forecast errors associated with a scalar stream function forecast error field ψ_k and a scalar velocity potential forecast error field χ_k (see Section 4.2.2).

Under the assumption that h_k, ψ_k, and χ_k are mutually independent, the cross terms in Eq. (26) are zero and we have

$$P_{ij}^{ua} := P_{ij}^h + P_{ij}^\psi + P_{ij}^\chi,\tag{31}$$

7

where

$$P_{ij}^h \quad := \quad < \vec{\epsilon}_i^h \vec{\epsilon}_j^{hT} >, \tag{32}$$

$$P_{ij}^\psi \quad := \quad < \vec{\epsilon}_i^\psi \vec{\epsilon}_j^{\psi T} >, \tag{33}$$

$$P_{ij}^\chi \quad := \quad < \vec{\epsilon}_i^\chi \vec{\epsilon}_j^{\chi T} > . \tag{34}$$

The following two sections derive error covariance models of Eqs. (32), (33), and (34) that are used in the software implementation of the PSAS.

4.2.1 Coupled Height-Wind Forecast Error Covariances

We describe the multivariate height-wind model for the error covariances in the context of the upper air analysis. The sea-level covariances are treated separately in Sec. 4.3. The coupled wind errors are modeled in terms of the height error by assuming the following linear relationship described in DAO (1996, Sec. 5.2.7.2.2.1):

$$u_k^h \quad = \quad \frac{g}{2\Omega a} \left(\alpha_{um_k} \partial_{m_k} h_k + \alpha_{ul_k} \partial_{l_k} h_k \right) \tag{35}$$

$$v_k^h \quad = \quad \frac{g}{2\Omega a} \left(\alpha_{vm_k} \partial_{m_k} h_k + \alpha_{vl_k} \partial_{l_k} h_k \right), \quad k = i, j, \tag{36}$$

where g is the acceleration due to gravity, Ω is the Earth's rotational angular velocity, a is the Earth's radius, and the coefficients α_{um_k}, α_{ul_k}, α_{vm_k}, and α_{vl_k} are tunable, spatially dependent, parameters.

Substituting Eqs. (35) and (36) into Eq. (28) gives the matrix formula

$$\vec{\epsilon}_k^h \quad := \quad \hat{\alpha}_k \hat{g} \vec{d}_k h_k, \quad k = i, j, \tag{37}$$

where

$$\hat{\alpha}_k \quad \equiv \quad \begin{bmatrix} 1 & 0 & 0 \\ 0 & \alpha_{um_k} & \alpha_{ul_k} \\ 0 & \alpha_{vm_k} & \alpha_{vl_k} \end{bmatrix}, \quad k = i, j, \tag{38}$$

$$\hat{g} \quad \equiv \quad \begin{bmatrix} 1 & 0 & 0 \\ 0 & \frac{g}{2\Omega a} & 0 \\ 0 & 0 & \frac{g}{2\Omega a} \end{bmatrix}, \tag{39}$$

and where $\vec{d}_k$ is the operator defined as follows:

$$\vec{d}_k f(\varphi_k, \lambda_k) \quad := \quad \begin{bmatrix} f(\varphi_k, \lambda_k) \\ \partial_{m_k} f(\varphi_k, \lambda_k) \\ \partial_{l_k} f(\varphi_k, \lambda_k) \end{bmatrix}, \quad k = i, j. \tag{40}$$

Using Eqn. (32), P_{ij}^h (a 3×3 matrix, not to be confused with Eqn. (25)) can be written as

$$P_{ij}^h \quad = \quad \hat{\alpha}_i \hat{g} \vec{d}_i (\vec{d}_j < h_i h_j >)^T \hat{g} \hat{\alpha}_j^T, \tag{41}$$

where we have taken the expectation inside the constants and the differential operators, and

$$\vec{d}_i(\vec{d}_j < h_i h_j >)^T \; = $$

$$\left[\begin{array}{ccc} < h_i h_j > & \partial_{m_j} < h_i h_j > & \partial_{l_j} < h_i h_j > \\ \partial_{m_i} < h_i h_j > & \partial_{m_i} \partial_{m_j} < h_i h_j > & \partial_{m_i} \partial_{l_j} < h_i h_j > \\ \partial_{l_i} < h_i h_j > & \partial_{l_i} \partial_{m_j} < h_i h_j > & \partial_{l_i} \partial_{l_j} < h_i h_j > \end{array} \right]. \tag{42}$$

Now using the same form as Eq. (25) we model the expectation as

$$< h_i h_j > = \sigma_i^h \rho_{ij}^h \sigma_j^h, \tag{43}$$

where σ_k^h is the forecast height error standard deviation, and where ρ_{ij}^h is the forecast height error correlation function.

By applying the product rule, we obtain:

$$\vec{d}_i \sigma_i^h \rho_{ij}^h \; = \; \sigma_i^h \left[\begin{array}{c} 1 \\ \partial_{m_i} \\ \partial_{l_i} \end{array} \right] \rho_{ij}^h + \rho_{ij}^h \left[\begin{array}{c} 0 \\ \partial_{m_i} \\ \partial_{l_i} \end{array} \right] \sigma_i^h, \tag{44}$$

which can be rewritten in matrix form as

$$\vec{d}_i \sigma_i^h \rho_{ij}^h \; = \; \tilde{\sigma}_i^h \vec{d}_i \rho_{ij}^h, \tag{45}$$

where

$$\tilde{\sigma}_i^h \; := \; \left[\begin{array}{ccc} \sigma_i^h & 0 & 0 \\ \partial_{m_i} \sigma_i^h & \sigma_i^h & 0 \\ \partial_{l_i} \sigma_i^h & 0 & \sigma_i^h \end{array} \right]. \tag{46}$$

Substituting Eqns. (43) and (45) in Eqn. (41) yields:

$$P_{ij}^h \; = \; \hat{\alpha}_i \hat{g} \tilde{\sigma}_i^h \vec{d}_i (\vec{d}_j \rho_{ij}^h)^T \tilde{\sigma}_j^{hT} \hat{g} \hat{\alpha}_j^T. \tag{47}$$

We now develop an explicit form for the correlation matrix $\vec{d}_i (\vec{d}_j \rho_{ij}^h)^T$ in expression (47). First, using the chain rule, and identities (16-19) for the polarity index τ_{ij}, we obtain:

$$\vec{d}_i \rho_{ij}^h = \left[\begin{array}{c} \rho_{ij}^h \\ \rho_{ij}^{h}{}' \tau_{ij}^{mr} \\ \rho_{ij}^{h}{}' \tau_{ij}^{lr} \end{array} \right], \tag{48}$$

where we denote

$$\rho_{ij}^{h}{}' \; := \; \frac{\partial \rho_{ij}^h}{\partial \tau_{ij}}. \tag{49}$$

We are assuming here, and in all our multivariate models, that the covariance functions are differentiable. Appendix B presents an illustration of how the differentiation may be evaluated termwise in a Legendre series.

Substitution of Eqn. (48) in $\vec{d}_i(\vec{d}_j\rho_{ij}^h)^T$ and use of the identities in Eqns. (20-23) yields:

$$\vec{d}_i(\vec{d}_j\rho_{ij}^h)^T \; = $$

$$\begin{bmatrix} \rho_{ij}^h & \rho_{ij}^{h\,'}\tau_{ij}^{rm} & \rho_{ij}^{h\,'}\tau_{ij}^{lr} \\ \rho_{ij}^{h\,'}\tau_{ij}^{mr} & \rho_{ij}^{h\,''}\tau_{ij}^{rm}\tau_{ij}^{mr} + \rho_{ij}^{h\,'}\tau_{ij}^{mm} & \rho_{ij}^{h\,''}\tau_{ij}^{rl}\tau_{ij}^{mr} + \rho_{ij}^{h\,'}\tau_{ij}^{ml} \\ \rho_{ij}^{h\,'}\tau_{ij}^{lr} & \rho_{ij}^{h\,''}\tau_{ij}^{rm}\tau_{ij}^{lr} + \rho_{ij}^{h\,'}\tau_{ij}^{lm} & \rho_{ij}^{h\,''}\tau_{ij}^{rl}\tau_{ij}^{lr} + \rho_{ij}^{h\,'}\tau_{ij}^{ll} \end{bmatrix}. \tag{50}$$

We finally normalize this correlation matrix by writing

$$\vec{d}_i(\vec{d}_j\rho_{ij}^h)^T \; = \; \hat{n}_i^h\hat{c}_{ij}^h\hat{n}_j^h, \tag{51}$$

where $\hat{n}_k^h = \mathrm{diag}\left[1, n_k^h, n_k^h\right]$, and

$$n_k^h \; := \; \sqrt{\frac{\partial}{\partial\tau}\rho^h(\tau,p_k,p_k)} \; \Big|_{\tau=1}, \quad k=i,j. \tag{52}$$

Appendix B shows that the argument of the square root is positive in the case that ρ^h is nonconstant.

Now Eqn. (47) can be written as a factored height-wind forecast error covariance function:

$$P_{ij}^h = \hat{\alpha}_i\hat{\sigma}_i^h\hat{c}_{ij}^h\hat{\sigma}_j^{hT}\hat{\alpha}_j^T, \tag{53}$$

where $\hat{\alpha}_i$ is given by Eq. (38), and

$$\hat{\sigma}_k^h \; = \; \hat{g}\tilde{\sigma}_k^h\hat{n}_k^h \; = \; \begin{bmatrix} \sigma_k^h & 0 & 0 \\ \frac{g\partial_{m_k}\sigma_k^h}{2\Omega a} & \frac{gn_k^h\sigma_k^h}{2\Omega a} & 0 \\ \frac{g\partial_{l_k}\sigma_k^h}{2\Omega a} & 0 & \frac{gn_k^h\sigma_k^h}{2\Omega a} \end{bmatrix}, \quad k=i,j. \tag{54}$$

The normalized correlation matrix is

$$\hat{c}_{ij}^h \; = \; \begin{bmatrix} c_{hh}^h & c_{hm}^h & c_{hl}^h \\ c_{mh}^h & c_{mm}^h & c_{ml}^h \\ c_{lh}^h & c_{lm}^h & c_{ll}^h \end{bmatrix}, \tag{55}$$

where

$$c_{hh}^h \; := \; \rho_{ij}^h \tag{56}$$

$$c_{mh}^h \; := \; (\partial_{m_i}\rho_{ij}^h)/n_i^h = \rho_{ij}^{h\,'}\tau_{ij}^{mr}/n_i^h \tag{57}$$

$$c_{hm}^h \; := \; (\partial_{m_j}\rho_{ij}^h)/n_j^h = \rho_{ij}^{h\,'}\tau_{ij}^{rm}/n_j^h \tag{58}$$

$$c_{lh}^h \; := \; (\partial_{l_i}\rho_{ij}^h)/n_i^h = \rho_{ij}^{h\,'}\tau_{ij}^{lr}/n_i^h \tag{59}$$

$$c_{hl}^h \; := \; (\partial_{l_j}\rho_{ij}^h)/n_j^h = \rho_{ij}^{h\,'}\tau_{ij}^{rl}/n_j^h \tag{60}$$

$$c_{mm}^h \; := \; (\partial_{m_i}\partial_{m_j}\rho_{ij}^h)/n_i^h n_j^h = (\rho_{ij}^{h\,''}\tau_{ij}^{rm}\tau_{ij}^{mr} + \rho_{ij}^{h\,'}\tau_{ij}^{mm})/n_i^h n_j^h \tag{61}$$

$$c_{lm}^h \; := \; (\partial_{l_i}\partial_{m_j}\rho_{ij}^h)/n_i^h n_j^h = (\rho_{ij}^{h\,''}\tau_{ij}^{rm}\tau_{ij}^{lr} + \rho_{ij}^{h\,'}\tau_{ij}^{lm})/n_i^h n_j^h \tag{62}$$

$$c_{ml}^h \; := \; (\partial_{l_i}\partial_{m_j}\rho_{ij}^h)/n_i^h n_j^h = (\rho_{ij}^{h\,''}\tau_{ij}^{rl}\tau_{ij}^{mr} + \rho_{ij}^{h\,'}\tau_{ij}^{ml})/n_i^h n_j^h \tag{63}$$

$$c_{ll}^h \; := \; (\partial_{l_i}\partial_{l_j}\rho_{ij}^h)/n_i^h n_j^h = (\rho_{ij}^{h\,''}\tau_{ij}^{rl}\tau_{ij}^{lr} + \rho_{ij}^{h\,'}\tau_{ij}^{ll})/n_i^h n_j^h. \tag{64}$$

By construction $c_{hh}^h = c_{mm}^h = c_{ll}^h = 1$ when $i = j$. Following the discussion in Appendix B, n_k^h is positive, i.e., there is no division by zero in Eqs. (56) - (64).

For the Optimal Interpolation algorithm of GEOS-1 DAS the equivalent matrix elements of Eq. (53) are evaluated explicitly (see Eqs. (19-26), (109-117) and (119-126) of Pfaendtner *et al.* 1995).

P_{ij}^h and $\hat{c}_{ij}^h$ are 3×3 matrices of functions of (τ_{ij}, p_i, p_j), $\hat{\alpha}_k$, and $\hat{\sigma}_k^h$ are 3×3 matrices of functions of $(\lambda_k, \varphi_k, p_k)$, ρ_{ij}^h is a function of (τ_{ij}, p_i, p_j), and n_k^h is a function of p_k.

For the PSAS v1.5.1, the horizontal gradients of the forecast error standard deviation are neglected, i.e., the implemented $\hat{\sigma}_k^h$ is diagonal. Also, tunable parameters in $\hat{\alpha}_k$ vary only in the latitude and pressure coordinates.

4.2.2   Decoupled Wind Forecast Error Covariances

Following the treatment in DAO (1996, Sec. 5.2.7.2.2) the remaining terms in the forecast error field, Eq. (27), arise from wind errors that are decoupled from the height field. The height-decoupled wind errors are formulated in terms of scalar stream function (ψ_k) and velocity potential (χ_k) error fields as follows:

$$u_k^\psi = -(\frac{g}{2\Omega a})\partial_{m_k}\psi_k \tag{65}$$

$$v_k^\psi = (\frac{g}{2\Omega a})\partial_{l_k}\psi_k \tag{66}$$

$$u_k^\chi = (\frac{g}{2\Omega a})\partial_{l_k}\chi_k \tag{67}$$

$$v_k^\chi = (\frac{g}{2\Omega a})\partial_{m_k}\chi_k, \quad k = i, j, \tag{68}$$

where ψ_k and χ_k are normalized to meters (i.e., the same units as the height error field).

We follow closely the development after Eq. (37) and find considerable economy of notation. The decoupled wind error fields (Eqs. (29) and (30)) may be written:

$$\vec{\epsilon}_k^\psi := \hat{\beta}\hat{g}\vec{d}_k\psi_k, \tag{69}$$

$$\vec{\epsilon}_k^\chi := \hat{\gamma}\hat{g}\vec{d}_k\chi_k, \quad k = i, j \tag{70}$$

where $\hat{g}$ is given by Eq. (39), $\vec{d}_k$ by Eq. (40), and

$$\hat{\beta} \equiv \begin{bmatrix} 0 & 0 & 0 \\ 0 & -1 & 0 \\ 0 & 0 & 1 \end{bmatrix}, \tag{71}$$

$$\hat{\gamma} \equiv \begin{bmatrix} 0 & 0 & 0 \\ 0 & 0 & 1 \\ 0 & 1 & 0 \end{bmatrix}. \tag{72}$$

The factored decoupled wind forecast error covariance functions are found in a manner similar to the previous section:

$$P_{ij}^\psi = \hat{\beta}\hat{\sigma}_i^\psi \hat{c}_{ij}^\psi \hat{\sigma}_j^{\psi T}\hat{\beta}^T, \tag{73}$$

$$P_{ij}^\chi = \hat{\gamma}\hat{\sigma}_i^\chi \hat{c}_{ij}^\chi \hat{\sigma}_j^{\chi T}\hat{\gamma}^T. \tag{74}$$

The error covariances of the stream function and velocity potential error fields are modeled similar to Eq. (43):

$$< \psi_i \psi_j > \quad = \quad \sigma_i^\psi \rho_{ij}^\psi \sigma_j^\psi, \tag{75}$$

$$< \chi_i \chi_j > \quad = \quad \sigma_i^\chi \rho_{ij}^\chi \sigma_j^\chi, \tag{76}$$

where σ_k^ψ and σ_k^χ are the forecast error standard deviation of the stream function and the velocity potential error fields, and where ρ_{ij}^ψ and ρ_{ij}^χ are the corresponding forecast error correlation functions.

In terms of the quantities in Eqs. (75) and (76), the matrices $\hat{\sigma}_k^\psi$ and $\hat{\sigma}_k^\chi$ are given in the same form as Eq. (54) with superscripts h replaced by ψ and χ respectively. Similarly, the correlation matrices $\hat{c}_{ij}^\psi$ and $\hat{c}_{ij}^\chi$ have the same form as Eqs. (55) to (64) with superscripts h replaced by ψ and χ respectively. By construction, only the lower right 2×2 submatrices of P_{ij}^ψ and P_{ij}^χ are nonzero.

For the PSAS v1.5.1, the horizontal gradients of the forecast error standard deviations are neglected, i.e., the implemented $\hat{\sigma}_k^\psi$ and $\hat{\sigma}_k^\chi$ are diagonal. For this case, only the lower right 2×2 submatrices of $\hat{c}_{ij}^\psi$ and $\hat{c}_{ij}^\chi$ are needed (and hence implemented) in the PSAS (Larson *et al.* 1998). This will have to be modified when horizontal gradients in the error standard deviation fields are implemented.

4.3   Multivariate Sea-level Forecast Error Covariances

The multivariate sea-level (*sl*) analysis is similar to the upper-air analysis with a coupled sea-level pressure and sea-level wind component (cf. Sec. 4.2.1) and a decoupled sea-level wind component that uses the same algorithm as the upper-air analysis (cf. Sec. 4.2.2).

The sea-level forecast error covariance function is defined as a 3×3 matrix:

$$P_{ij}^{sl} := < \vec{\epsilon}_i^{sl} \vec{\epsilon}_j^{slT} >, \tag{77}$$

where $\vec{\epsilon}_k^{sl}$ $(k = i, j)$ is the forecast sea-level error field, which is comprised of three terms

$$\vec{\epsilon}_k^{sl} := \vec{\epsilon}_k^p + \vec{\epsilon}_k^\psi + \vec{\epsilon}_k^\chi, \quad k = i, j, \tag{78}$$

where

$$\vec{\epsilon}_k^p := \begin{bmatrix} p_k \\ u_k^p \\ v_k^p \end{bmatrix}, \quad k = i, j, \tag{79}$$

is a vector of sea-level pressure forecast error (p_k) and surface-pressure coupled wind forecast errors (u_k^p, u_k^p), and $\vec{\epsilon}_k^\psi$ and $\vec{\epsilon}_k^\chi$ are given by Eqs. (29) and (30).

The sea-level covariance formulation is linked to the upper-air analysis by using the hydrostatic balance condition to relate the pressure error field to the height error field:

$$p_k = -g\rho h_k, \quad k = i, j, \tag{80}$$

where h_k is the height error field at the sea surface. Once again, taking p_k (i.e., h_k), ψ_k and χ_k to be mutually independent:

$$P_{ij}^{sl} \quad := \quad P_{ij}^p + P_{ij}^\psi + P_{ij}^\chi, \tag{81}$$

where

$$P^p_{ij} := < \vec{\epsilon}^{\,p}_i \vec{\epsilon}^{\,pT}_j >, \tag{82}$$

and the decoupled sea-level wind forecast error covariance functions P^ψ_{ij} and P^χ_{ij} are defined in Eqs. (33) and (34). The factored operator models for P^ψ_{ij} and P^χ_{ij} are Eqs. (73) and (74), hence it is only necessary to derive the factored operator model for P^p_{ij}.

Following Eqs. (35) and (36) and the subsequent analysis, we derive the sea-level wind error fields in terms of the height error field at sea-level

$$u^p_k = \frac{g}{2\Omega a \rho_k} \left(\alpha_{um_k} \partial_{m_k} (\rho_k h_k) + \alpha_{ul_k} \partial_{l_k} (\rho_k h_k) \right) \tag{83}$$

$$v^p_k = \frac{g}{2\Omega a \rho_k} \left(\alpha_{vm_k} \partial_{m_k} (\rho_k h_k) + \alpha_{vl_k} \partial_{l_k} (\rho_k h_k) \right), \quad k = i, j. \tag{84}$$

Continuing almost the same analysis as in Section 4.2.1, we obtain the sea-level pressure-wind forecast error covariance model:

$$P^p_{ij} = \hat{\alpha}_i \hat{\sigma}^p_i \hat{c}^h_{ij} \hat{\sigma}^{pT}_j \hat{\alpha}^T_j, \tag{85}$$

where $\hat{\alpha}_k$ is given by Eq. (38), $\hat{c}^h_{ij}$ is given by Eqs. (55) to (64), and

$$\hat{\sigma}^p_k = \begin{bmatrix} g\rho_k \sigma^h_k & 0 & 0 \\ \frac{g \partial_{m_k}(\rho_k \sigma_k{}^h)}{2\Omega a \rho_k} & \frac{g n^h_k \sigma^h_k}{2\Omega a} & 0 \\ \frac{g \partial_{l_k}(\rho_k \sigma^h_k)}{2\Omega a \rho_k} & 0 & \frac{g n^h_k \sigma^h_k}{2\Omega a} \end{bmatrix}. \tag{86}$$

For the PSAS v1.5.1, the horizontal gradients in Eq. (86) are neglected, i.e., the implemented $\hat{\sigma}^p_k$ is diagonal (cf. Sec. 4.2.2). Also, the sea-level air densities ρ_k are approximated by $\bar{\rho} = 1.24$ kg/m^3 and $\hat{\alpha}_k$, $\hat{\sigma}^p_k$, and $\hat{c}^h_{ij}$ are evaluated at the 1000 hPa level.

The matrices $\hat{\alpha}_k$, $\hat{\sigma}^h_k$, $\hat{\sigma}^\psi_k$, $\hat{\sigma}^\chi_k$, $\hat{c}^h_{ij}$, $\hat{c}^\psi_{ij}$, and $\hat{c}^\chi_{ij}$ are common to the upper air and the sea-level analyses. In the implementation of the PSAS, the actual values of the parameters that are input to these quantities are level dependent, and this is how the sea-level quantities are different from their upper-air values.

5 Observation Error Covariance Models

The observation error covariance matrix R in Eq. (1) is implemented using univariate covariance models. There are three classes of models:

Class I: The observation errors are independent. Given observations at i and j, the entry in the observation error covariance matrix is:

$$R_{ij} = \sigma_{oi} \sigma_{oj} \delta_{ij}, \tag{87}$$

where δ_{ij} is the Kronecker delta, and σ_{ok}, for $k = i, j$, is the observation error standard deviation. Examples of observations that are independent include:

- Surface station observations

- Cloud-track winds

- Aircraft observations.

Class II: The observation errors are vertically correlated within the same profile:

$$R_{ij} = \sigma_{oui}\sigma_{ouj}\nu_{ou}(p_i, p_j)\delta_{\mathbf{kt}_i,\mathbf{kt}_j}\delta_{\mathbf{kx}_i,\mathbf{kx}_j}\delta_{\mathbf{ks}_i,\mathbf{ks}_j}, \tag{88}$$

where $\delta_{\mathbf{kt}_i,\mathbf{kt}_j}$, $\delta_{\mathbf{kx}_i,\mathbf{kx}_j}$, and $\delta_{\mathbf{ks}_i,\mathbf{ks}_j}$ are Kronecker deltas over the data type, data source, and profile indices, respectively. The subscript u indicates that these observations are horizontally uncorrelated. The quantity $\nu_{ou}(p_i, p_j)$ is the vertical correlation coefficient. Examples of observations in this class include:

- Rawinsonde observations

- Rocketsonde observations

- Dropwinsonde observations.

Class III: The observation errors consist of two components, one of which is horizontally uncorrelated:

$$R_{ij} = \sigma_{oui}\sigma_{ouj}\nu_{ou}(p_i, p_j)\delta_{\mathbf{kt}_i,\mathbf{kt}_j}\delta_{\mathbf{kx}_i,\mathbf{kx}_j} + \sigma_{oci}\sigma_{ocj}\rho_{oc}(\tau_{ij}, p_i, p_j)\delta_{\mathbf{kt}_i,\mathbf{kt}_j}\delta_{\mathbf{kx}_i,\mathbf{kx}_j}, \tag{89}$$

where the subscript c indicates a horizontal correlation between i and j. Currently, the only observation class processed by the PSAS that uses this covariance model is TOVS satellite heights data.

6   Implementation of the PSAS

In this section we will outline the software implementation of the PSAS, drawing attention to the form of the factored matrices, and commenting on the implications for computational and software complexity. The discussion will describe the matrices of the PSAS, but it should be noted that actual matrices are never formed in the PSAS, rather they are implemented in operator form as outlined in Appendix C. This is described in greater detail in Larson *et al.* (1998).

6.1   Decomposition of the PSAS Grids

The structure of matrices in the PSAS is dictated by the specific decomposition of the observational and analysis grids within the software. We describe this decomposition in this section.

For the PSAS v1.5.1, the innovation vectors are sorted according to the following hierarchy of their attributes:

- region index `kr`

- physical variable class `kt`

- instrument class `kx`

- latitude φ

- longitude λ

- pressure level `kz`

The first two levels of this hierarchy – sort over `kr-kt` – are relevant to the present discussion. Analysis grid points are sorted over `kr-kt`.

Currently, the region index `kr` for a point is based its latitude and longitude. For the innovations, the surface of the sphere is divided into 80 regions through an icosahedral partitioning scheme, with each region corresponding to a value of `kr` (Pfaendtner 1996). Thus the error covariance matrices are each divided into 6400 regions. The analysis grid points have an equal area regional decomposition with 80 regions.

Sorting the globe into $\mathcal{N}_r$ regions for innovations and analysis grid points yields:

$$\mathbf{w^o} = \left[\begin{array}{c} \mathbf{w^o}_1 \\ \vdots \\ \mathbf{w^o}_{\mathcal{N}_r} \end{array} \right] \quad \mathbf{x} = \left[\begin{array}{c} \mathbf{x}_1 \\ \vdots \\ \mathbf{x}_{\mathcal{N}_r} \end{array} \right] \quad \mathbf{w^a} = \left[\begin{array}{c} \mathbf{w^a}_1 \\ \vdots \\ \mathbf{w^a}_{\mathcal{N}_r} \end{array} \right] . \tag{90}$$

If $\mathbf{w^o}, \mathbf{x} \in I\!\!R^p$, and $\mathbf{w^a} \in I\!\!R^n$, then $\mathbf{w^o}_i, \mathbf{x}_i \in I\!\!R^{p_i}$, where $\sum_{i=1}^{\mathcal{N}_r} p_i = p$, and $\mathbf{w^a}_i \in I\!\!R^{n_i}$, where $\sum_{i=1}^{\mathcal{N}_r} n_i = n$. Within each of the regional vectors $\mathbf{w^o}_i$, $\mathbf{x}_i$, and $\mathbf{w^a}_i$ the elements are sorted by `kt`.

6.2 Formulation of $HP^f H^T$ and $P^f H^T$

The forecast error covariance matrix appears in the innovation equation as $HP^f H^T$, and in the analysis equation as $P^f H^T$. The analysis equations of the PSAS are solved for three different groups of observations (relevant equation numbers from the text are given in parenthesis):

- Mixing ratio analysis: P_{ij}^z, $z \equiv q$ (25)

- Sea-level pressure-wind analysis: P_{ij}^p (85), P_{ij}^ψ (73), P_{ij}^χ (74)

- Upper-air height-wind analysis: P_{ij}^h (53), P_{ij}^ψ (73), P_{ij}^χ (74)

The general form for the components of $HP^f H^T$ or $P^f H^T$ for the multivariate sea-level and upper-air analysis is:

$$P = \Gamma_L \Sigma_L C \Sigma_R^T \Gamma_R^T, \tag{91}$$

where the matrices $\Gamma_L, \Sigma_L, \Gamma_R$, and Σ_R are block-diagonal matrices, and C is (in principle) dense. These matrices are grid evaluations of the component matrices defined in Eqns. (25), (53), (73), (74), and (85) (i.e., from the above list). For the case $P^f H^T$, the matrices Γ_L (Γ_R) and Σ_L (Σ_R) are $n_{\mathbf{kt}} \times n_{\mathbf{kt}}$ ($p_{\mathbf{kt}} \times p_{\mathbf{kt}}$), and C is $n_{\mathbf{kt}} \times p_{\mathbf{kt}}$, where $p_{\mathbf{kt}}$ is the number of observations depending on whether the analysis is sea-level or upper-air, and $n_{\mathbf{kt}}$ is the number of analysis grid points. For the case $HP^f H^T$, the matrices Γ_L, Γ_R, Σ_L, Σ_R, and

C are $p_{\mathbf{kt}} \times p_{\mathbf{kt}}$. For the upper-air height-wind analysis, the *global* forecast error covariance matrix is the sum of height-wind and decoupled wind matrices of the form (91):

$$
\begin{aligned}
P^{ua} &= P^h + P^\psi + P^\chi \\
&= \Gamma_L^h \Sigma_L^h C'^h \Sigma_R^{hT} \Gamma_R^{hT} + \Gamma_L^\psi \Sigma_L^\psi C'^\psi \Sigma_R^{\psi T} \Gamma_R^{\psi T} \\
&\quad + \Gamma_L^\chi \Sigma_L^\chi C'^\chi \Sigma_R^{\chi T} \Gamma_R^{\chi T}
\end{aligned} \quad . \tag{92}
$$

The Γ matrices are regional (`kr`) block-diagonal:

$$
\Gamma = \begin{bmatrix}
\Gamma_1 & \mathbf{0} & \cdots & \mathbf{0} \\
\mathbf{0} & \ddots & \ddots & \vdots \\
\vdots & \ddots & \ddots & \mathbf{0} \\
\mathbf{0} & \cdots & \mathbf{0} & \Gamma_{\mathcal{N}_r}
\end{bmatrix} , \tag{93}
$$

where each `kr` block is formed of 3×3 (`kt-kt`) sub-blocks. For the height-wind analysis, the data are sorted over type in the order (h, u, v). With this, the ith `kr` block of Γ^h is:

$$
\Gamma_i^h = \left[
\begin{array}{ccc|ccc|ccc}
1 & \cdots & 0 & 0 & \cdots & 0 & 0 & \cdots & 0 \\
\vdots & \ddots & \ddots & \ddots & \ddots & \ddots & \ddots & \ddots & \vdots \\
0 & \ddots & 1 & 0 & \ddots & 0 & 0 & \ddots & 0 \\
\hline
0 & \ddots & 0 & \alpha_{um_1} & \ddots & 0 & \alpha_{ul_1} & \ddots & 0 \\
\vdots & \ddots & \ddots & \ddots & \ddots & \ddots & \ddots & \ddots & \vdots \\
0 & \ddots & 0 & 0 & \ddots & \alpha_{um_{s_i}} & 0 & \ddots & \alpha_{ul_{s_i}} \\
\hline
0 & \ddots & 0 & \alpha_{vm_1} & \ddots & 0 & \alpha_{vl_1} & \ddots & 0 \\
\vdots & \ddots & \ddots & \ddots & \ddots & \ddots & \ddots & \ddots & \vdots \\
0 & \cdots & 0 & 0 & \cdots & \alpha_{vm_{s_i}} & 0 & \cdots & \alpha_{vl_{s_i}}
\end{array}
\right] , \tag{94}
$$

where s_i is the number of (h, u, v) members in the region i, and the grid-evaluated elements are, for instance, $\alpha_{um_q} = \alpha_{um}(\lambda_q, \varphi_q, p_q)$, see Eqs. (35) and (36). The ith `kr` blocks of Γ^ψ and Γ^χ are:

$$
\Gamma_i^{\psi} =
\left[
\begin{array}{ccc|ccc|ccc}
0 & \cdots & 0 & 0 & \cdots & 0 & 0 & \cdots & 0 \\
\vdots & \ddots & \ddots & \ddots & \ddots & \ddots & \ddots & \ddots & \vdots \\
0 & \ddots & 0 & 0 & \ddots & 0 & 0 & \ddots & 0 \\
\hline
0 & \ddots & 0 & -1 & \ddots & 0 & 0 & \ddots & 0 \\
\vdots & \ddots & \ddots & \ddots & \ddots & \ddots & \ddots & \ddots & \vdots \\
0 & \ddots & 0 & 0 & \ddots & -1 & 0 & \ddots & 0 \\
\hline
0 & \ddots & 0 & 0 & \ddots & 0 & 1 & \ddots & 0 \\
\vdots & \ddots & \ddots & \ddots & \ddots & \ddots & \ddots & \ddots & \vdots \\
0 & \cdots & 0 & 0 & \cdots & 0 & 0 & \cdots & 1
\end{array}
\right] ,
\tag{95}
$$

$$
\Gamma_i^{\chi} =
\left[
\begin{array}{ccc|ccc|ccc}
0 & \cdots & 0 & 0 & \cdots & 0 & 0 & \cdots & 0 \\
\vdots & \ddots & \ddots & \ddots & \ddots & \ddots & \ddots & \ddots & \vdots \\
0 & \ddots & 0 & 0 & \ddots & 0 & 0 & \ddots & 0 \\
\hline
0 & \ddots & 0 & 0 & \ddots & 0 & 1 & \ddots & 0 \\
\vdots & \ddots & \ddots & \ddots & \ddots & \ddots & \ddots & \ddots & \vdots \\
0 & \ddots & 0 & 0 & \ddots & 0 & 0 & \ddots & 1 \\
\hline
0 & \ddots & 0 & 1 & \ddots & 0 & 0 & \ddots & 0 \\
\vdots & \ddots & \ddots & \ddots & \ddots & \ddots & \ddots & \ddots & \vdots \\
0 & \cdots & 0 & 0 & \cdots & 1 & 0 & \cdots & 0
\end{array}
\right] .
\tag{96}
$$

Like Γ, the Σ matrices are block diagonal:

$$
\Sigma =
\left[
\begin{array}{cccc}
\Sigma_1 & \mathbf{0} & \cdots & \mathbf{0} \\
\mathbf{0} & \ddots & \ddots & \vdots \\
\vdots & \ddots & \ddots & \mathbf{0} \\
\mathbf{0} & \cdots & \mathbf{0} & \Sigma_{\mathcal{N}_r}
\end{array}
\right] ,
\tag{97}
$$

where for the height-wind analysis, the ith `kr` block of Σ^h is:

$$
\Sigma_i^h =
\left[
\begin{array}{ccc|ccc|ccc}
\sigma_1^h & \cdots & 0 & 0 & \cdots & 0 & 0 & \cdots & 0 \\
\vdots & \ddots & \ddots & \ddots & \ddots & \ddots & \ddots & \ddots & \vdots \\
0 & \ddots & \sigma_{s_i}^h & 0 & \ddots & 0 & 0 & \ddots & 0 \\
\hline
A\partial_m\sigma_1^h & \ddots & 0 & An_1^h\sigma_1^h & \ddots & 0 & 0 & \ddots & 0 \\
\vdots & \ddots & \ddots & \ddots & \ddots & \ddots & \ddots & \ddots & \vdots \\
0 & \ddots & A\partial_m\sigma_{s_i}^h & 0 & \ddots & An_{s_i}^h\sigma_{s_i}^h & 0 & \ddots & 0 \\
\hline
A\partial_l\sigma_1^h & \ddots & 0 & 0 & \ddots & 0 & An_1^h\sigma_1^h & \ddots & 0 \\
\vdots & \ddots & \ddots & \ddots & \ddots & \ddots & \ddots & \ddots & \vdots \\
0 & \cdots & A\partial_l\sigma_{s_i}^h & 0 & \cdots & 0 & 0 & \cdots & An_{s_i}^h\sigma_{s_i}^h
\end{array}
\right] , \quad (98)
$$

and Σ_i^ψ and Σ_i^χ are the same form as Σ_i^h with h replaced by ψ and χ respectively, and $A = g/(2\Omega a)$.

The `kr` blocks (Γ_i^h, Γ_i^ψ, Γ_i^χ, Σ_i^h, Σ_i^ψ, and Σ_i^χ) are themselves sparse. This matrix representation should not be confused with the software implementation which only loops over non-zero elements.

The block matrix C is dense:

$$
C =
\left[
\begin{array}{ccccc}
C_{1,1} & C_{1,2} & \cdots & C_{1,\mathcal{N}_r-1} & C_{1,\mathcal{N}_r} \\
C_{2,1} & C_{2,2} & \cdots & C_{2,\mathcal{N}_r-1} & C_{2,\mathcal{N}_r} \\
\vdots & \vdots & \ddots & \vdots & \vdots \\
C_{\mathcal{N}_r-1,1} & C_{\mathcal{N}_r-1,2} & \cdots & C_{\mathcal{N}_r-1,\mathcal{N}_r-1} & C_{\mathcal{N}_r-1,\mathcal{N}_r} \\
C_{\mathcal{N}_r,1} & C_{\mathcal{N}_r,2} & \cdots & C_{\mathcal{N}_r,\mathcal{N}_r-1} & C_{\mathcal{N}_r,\mathcal{N}_r}
\end{array}
\right] , \quad (99)
$$

where the $i^{\text{th}} \times j^{\text{th}}$ `kr-kr` block of C^h is:

$$
C_{ij}^h =
\left[
\begin{array}{ccc|ccc|ccc}
C_{h1h1}^h & \cdots & C_{h1hs_j}^h & C_{h1m1}^h & \cdots & C_{h1ms_j}^h & C_{h1l1}^h & \cdots & C_{h1ls_j}^h \\
\vdots & \ddots & \ddots & \ddots & \ddots & \ddots & \ddots & \ddots & \vdots \\
C_{hs_ih1}^h & \ddots & C_{hs_ihs_j}^h & C_{hs_im1}^h & \ddots & C_{hs_ims_j}^h & C_{hs_il1}^h & \ddots & C_{hs_ils_j}^h \\
\hline
C_{m1h1}^h & \ddots & C_{m1hs_j}^h & C_{m1m1}^h & \ddots & C_{m1ms_j}^h & C_{m1l1}^h & \ddots & C_{m1ls_j}^h \\
\vdots & \ddots & \ddots & \ddots & \ddots & \ddots & \ddots & \ddots & \vdots \\
C_{ms_ih1}^h & \ddots & C_{ms_ihs_j}^h & C_{ms_im1}^h & \ddots & C_{ms_ims_j}^h & C_{ms_il1}^h & \ddots & C_{ms_ils_j}^h \\
\hline
C_{l1h1}^h & \ddots & C_{l1hs_j}^h & C_{l1m1}^h & \ddots & C_{l1ms_j}^h & C_{l1l1}^h & \ddots & C_{l1ls_j}^h \\
\vdots & \ddots & \ddots & \ddots & \ddots & \ddots & \ddots & \ddots & \vdots \\
C_{ls_ih1}^h & \cdots & C_{ls_ihs_j}^h & C_{ls_im1}^h & \cdots & C_{ls_ims_j}^h & C_{ls_il1}^h & \cdots & C_{ls_ils_j}^h
\end{array}
\right] , \quad (100)
$$

where the grid-evaluated elements are, for instance, $C_{hqhr}^h = c_{hh}^h(\tau_{qr}, p_q, p_r)$, see Eqs. (56)-(64). The matrix blocks C_{ij}^ψ and C_{ij}^χ are the same form as C_{ij}^h with h replaced by ψ and χ

respectively.

The global sea-level forecast error covariance matrix is similar to the height-wind, except the data are sorted over type in the order (p_{sl}, u_{sl}, v_{sl}).

By using appropriately scaled compactly-supported correlation functions (Gaspari and Cohn 1999), blocks associated with regions separated by more than 6,030 km may be taken to be zero (DAO 1996). This introduces a coarse-grained sparsity into C that reduces the computational complexity.

The univariate global mixing ratio forecast error covariance matrix is a trivial software implementation of (91), illustrating that the traditional decomposition of a covariance function into a product of standard deviation terms and a correlation function is the simplest form of the factored operator approach:

$$P^q = \Sigma_L^q C^q \Sigma_R^{qT} . \tag{101}$$

In the PSAS, the horizontally correlated part of the observation error covariance matrix R (Eq. 89) is treated the same as the univariate forecast error matrix software implementation. Independent observations (Class I) contribute only diagonal matrix elements, while observations with vertically correlated profiles in Class II and III contribute matrix elements that are derived from vertical correlation coefficients.

Section 6.3 discusses the modification to the above matrices for the case where observations do not occur in triplets (h, u, v).
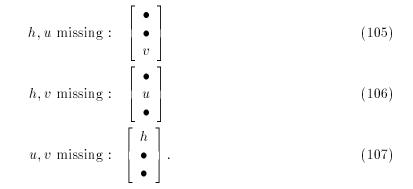
Two key consequences of sorting by `kr-kt` are:

- Sorting by `kr` enables coarse-grained sparsity to be applied to the correlation matrices $C^{h,\psi,\chi}$, using the 6,030 km cutoff, which reduces the computational complexity.

- Sorting by `kt` within each region generates `kt-kt` sub-blocks whose software implementations use homogeneous data types, thus enabling modular software (Larson *et al.* 1998).

6.3   Dealing with Missing Data in Multivariate Observations

The height-wind and sea-level pressure-wind forecast error covariance models derived in Section 4 and further discussed in Sections 6.1 and 6.2 assumed no missing data in the triplets (h, u, v) and (p_{sl}, u_{sl}, v_{sl}).

For the upper-air height-wind analysis, let the bullet symbol (•) represent a missing observation. For a given point, all the possible combinations of missing observations are:

$$h \text{ missing} : \begin{bmatrix} \bullet \\ u \\ v \end{bmatrix} \tag{102}$$

$$u \text{ missing} : \begin{bmatrix} h \\ \bullet \\ v \end{bmatrix} \tag{103}$$

$$v \text{ missing} : \begin{bmatrix} h \\ u \\ \bullet \end{bmatrix} \tag{104}$$

$$h, u \text{ missing} : \quad \begin{bmatrix} \bullet \\ \bullet \\ v \end{bmatrix} \tag{105}$$

$$h, v \text{ missing} : \quad \begin{bmatrix} \bullet \\ u \\ \bullet \end{bmatrix} \tag{106}$$

$$u, v \text{ missing} : \quad \begin{bmatrix} h \\ \bullet \\ \bullet \end{bmatrix}. \tag{107}$$

For the PSAS v1.5.1, only cases (102) and (107) are implemented; the listing of the other cases is for completeness.

Consider the contribution of P^h_{ij}, Eq. (53) in the innovation equation (1). Blocks $\hat{\alpha}_i$ and $\hat{\sigma}^h_i$, are affected only by missing observations at point i, and the blocks $\hat{\alpha}_j$ and $\hat{\sigma}^h_j$, are affected only by missing observations at point j. Table 1 summarizes the structure of the matrix block $\hat{\alpha}_i$ for the missing observation cases defined in (102-107).

A missing observation in the triple (h, u, v) at i or j corresponds to removal of the corresponding row or column respectively in $\hat{\mathbf{c}}^h_{ij}$. A summary of the dimensions of $\hat{\mathbf{c}}^h_{ij}$ for various combinations of missing observations is presented in Table 2. Once again, note that the majority of the cases listed in this table are not implemented, and are presented for completeness.

7   Discussion

This document describes the theoretical basis for the software implementation of the PSAS v1.5.1. The software is used in the production GEOS DAS algorithm at the DAO. Versions of PSAS under development include: forward observation operators, advanced covariance models, advanced Fortran 90 features, and the ability to run on parallel distributed-memory computers using the Message Passing Interface (MPI).

Table 1: Effect of Missing Observations on the Matrix Block $\hat{\alpha}_i$.

Case	$\hat{\alpha}_{\mathbf{i}}$	Dimensions	Implemented?
huv y	$\begin{bmatrix} 1 & 0 & 0 \\ 0 & \alpha_{um_i} & \alpha_{ul_i} \\ 0 & \alpha_{vm_i} & \alpha_{vl_i} \end{bmatrix}$	3×3	Yes
$\bullet uv$	$\begin{bmatrix} \bullet & \bullet & \bullet \\ \bullet & \alpha_{um_i} & \alpha_{ul_i} \\ \bullet & \alpha_{vm_i} & \alpha_{vl_i} \end{bmatrix}$	2×2	Yes
$h \bullet v$	$\begin{bmatrix} 1 & \bullet & 0 \\ \bullet & \bullet & \bullet \\ 0 & \bullet & \alpha_{vl_i} \end{bmatrix}$	2×2	No
$hu\bullet$	$\begin{bmatrix} 1 & 0 & \bullet \\ 0 & \alpha_{um_i} & \bullet \\ \bullet & \bullet & \bullet \end{bmatrix}$	2×2	No
$\bullet\bullet v$	$\begin{bmatrix} \bullet & \bullet & \bullet \\ \bullet & \bullet & \bullet \\ \bullet & \bullet & \alpha_{vl_i} \end{bmatrix}$	1×1	No
$h \bullet\bullet$	$\begin{bmatrix} 1 & \bullet & \bullet \\ \bullet & \bullet & \bullet \\ \bullet & \bullet & \bullet \end{bmatrix}$	1×1	Yes
$\bullet u\bullet$	$\begin{bmatrix} \bullet & \bullet & \bullet \\ \bullet & \alpha_{um_i} & \bullet \\ \bullet & \bullet & \bullet \end{bmatrix}$	1×1	No

Table 2: Dimensions of the Error Correlation Matrix Block $\hat{\mathbf{c}}_{ij}^h$

	huv	$\bullet uv$	$h \bullet v$	$hu\bullet$	$\bullet \bullet v$	$h \bullet \bullet$	$\bullet u\bullet$
huv	3×3	3×2	3×2	3×2	3×1	3×1	3×1
$\bullet uv$	2×3	2×2	2×2	2×2	2×1	2×1	2×1
$h \bullet v$	2×3	2×2	2×2	2×2	2×1	2×1	2×1
$hu\bullet$	2×3	2×2	2×2	2×2	2×1	2×1	2×1
$\bullet \bullet v$	1×3	1×2	1×2	1×2	1×1	1×1	1×1
$h \bullet \bullet$	1×3	1×2	1×2	1×2	1×1	1×1	1×1
$\bullet u\bullet$	1×3	1×2	1×2	1×2	1×1	1×1	1×1

Appendix A. Comparison of Computational Complexity of the Operator Approach versus Explicit Matrix Evaluation

To illustrate the difference between the computational complexity of the operator approach versus explicit evaluation of the matrix we will consider a simple, univariate example. Consider the case of evaluating Px, where $P = \Sigma C \Sigma^T$, where C is a dense $p \times p$ correlation matrix, and $\Sigma = \text{diag}[\sigma_1, \sigma_2, ..., \sigma_p]$. Assume that the elements of C are precalculated. Evaluating the $\frac{1}{2}p(p+1)$ nonredundant elements of P directly takes $p(p+1)$ floating point multiplies (i.e., $P_{ij} = \sigma_i C_{ij} \sigma_j$). It takes $2p^2$ flops (counting $+$ and $*$ each as a flop) to evaluate Px, for a total of $3p^2 + p$ flops. In contrast, evaluating $\Sigma^T x$, then $C(\Sigma^T x)$ then $\Sigma(C\Sigma^T x)$ takes p, $2p^2$, and p flops respectively for a total of $2p^2 + 2p$ flops. For this example, the operator approach saves approximately p^2 flops.

Appendix B. Differentiating a Correlation Function

Each differentiable function ρ_{ij}^h that represents a correlation function on the globe can be expanded into a Legendre series:

$$\rho_{ij}^h := \rho_{ij}^h(\tau_{ij}, p_i, p_j) = \sum_{m=0}^{\infty} a_m(p_i, p_j) P_m(\tau_{ij}), \quad \tau_{ij} \in [-1, 1] \tag{108}$$

where P_m is the $m-$th Legendre polynomial. If $k := i = j$, then $a_m(p_k, p_k) \geq 0$ for each m, and

$$\sum_{m=0}^{\infty} a_m(p_k, p_k) = 1 \tag{109}$$

(cf. Gaspari and Cohn 1999, Theorem 2.11). Termwise differentiation of Eqn. (108) yields:

$$\rho_{ij}^h{}' := \sum_{m=0}^{\infty} a_m(p_i, p_j) P_m{}'(\tau_{ij}), \quad \tau_{ij} \in [-1, 1]. \tag{110}$$

Note that since $P_m'(1) > 0$ and $a_m(p_k, p_k) \geq 0$ for each positive integer m, we have $\rho_{kk}^h{}'(1) \geq 0$. Since ρ_{ij}^h is nonconstant, Eqn. (109), the fact that $a_m(p_k, p_k) \geq 0$ for each positive integer m implies that $a_l(p_k, p_k) > 0$ for some $l > 0$. Since $P_l'(1) > 0$ and $a_l(p_k, p_k) > 0$ it follows that $\rho_{kk}^h{}' > 0$.

Appendix C. Applications of the Factored-Operator Formulation in the Solver and the Analysis Equation

The innovation equation (1) is solved using a preconditioned conjugate gradient (PCG) method (da Silva and Guo 1996, Cohn *et al.* 1998). Each step of the PCG solvers and CG preconditioners evaluate matrix-vector products of the form $(HP^f H^T + R)\mathbf{x}$. The analysis equation (2) evaluates $P^f H^T \mathbf{x}$. Following the discussion in Section 6, factored-operator

expressions for HP^fH^T or P^fH^T for the three analyses of the PSAS v1.5.1 may be summarized:

Upper-Air Height-Wind Analysis:

$$
\begin{aligned}
P^{ua} &= \Gamma_L^h\Sigma_L^h C^h\Sigma_R^{hT}\Gamma_R^{hT} + \Gamma_L^\psi\Sigma_L^\psi C^\psi\Sigma_R^{\psi T}\Gamma_R^{\psi T} \\
&+ \Gamma_L^\chi\Sigma_L^\chi C^\chi\Sigma_R^{\chi T}\Gamma_R^{\chi T}
\end{aligned} \quad .
\tag{111}
$$

Sea-Level Pressure-Wind Analysis:

$$
\begin{aligned}
P^{sl} &= \Gamma_L^p\Sigma_L^p C^p\Sigma_R^{pT}\Gamma_R^{pT} + \Gamma_L^\psi\Sigma_L^\psi C^\psi\Sigma_R^{\psi T}\Gamma_R^{\psi T} \\
&+ \Gamma_L^\chi\Sigma_L^\chi C^\chi\Sigma_R^{\chi T}\Gamma_R^{\chi T}
\end{aligned} \quad .
\tag{112}
$$

Upper-Air Mixing Ratio Analysis:

$$
P^q = \Sigma_L^q C^q\Sigma_R^{qT} \ .
\tag{113}
$$

The observation error covariance is of the form

$$
\begin{aligned}
R &= R_u + R_c \\
&= \Sigma_u^o C_u^o\Sigma_u^{oT} + \Sigma_c^o C_c^o\Sigma_c^{oT}
\end{aligned} \quad .
\tag{114}
$$

For each of the analyses of PSAS the quantity $\Gamma_L\Sigma_L C\Sigma_R^T\Gamma_R^T\mathbf{x}$ is evaluated in the following steps, each of which corresponds to a different subroutine:

$$
\begin{aligned}
\mathbf{x^a} &= \Gamma_R^T\mathbf{x} \\
\mathbf{x^b} &= \Sigma_R^T\mathbf{x^a} \\
\mathbf{x^c} &= C\mathbf{x^b} \\
\mathbf{x^d} &= \Sigma_L\mathbf{x^c} \\
\mathbf{x^e} &= \Gamma_L\mathbf{x^d}.
\end{aligned}
\tag{115}
$$

The operations $P^q\mathbf{x}$ (moisture analysis) and $R_c\mathbf{x}$ are similar to Eq. (115) but take three stages.

The solver for the innovation equation has three levels of preconditioners as follows:

- The regional preconditioner uses only the regional diagonal blocks of the correlation matrices C.

- The regional-univariate preconditioner uses only the regional-univariate blocks of C.

- The sounding-diagonal preconditioner performs a direct Cholesky solve using sounding-diagonal blocks of C.

For the innovation equation, the left and right matrices $\Gamma_{L,R}$ and $\Sigma_{L,R}$ are constructed from parameters evaluated at observation locations, and the correlation matrices C are evaluated on the Cartesian product of the observation locations. For the analysis equation, the matrices Γ_L, and Σ_L are constructed from parameters evaluated at analysis grid locations, while Γ_R, and Σ_R are constructed from parameters evaluated at observation locations. The correlation matrices C are evaluated on the Cartesian product of the analysis and observation locations.

Acknowledgments

References

Arfken, G., 1970: *Mathematical Methods for Physicists.* Academic Press, New York, 815 pp.

Cohn, S. E., A. da Silva, J. Guo, M. Sienkiewicz, and D. Lamich, 1998: Assessing the effects of data selection with the DAO Physical-space Statistical Analysis System. *Mon. Wea. Rev.,* **126**, 2913–2926.

Courtier, P., E. Andersson, W. Heckley, J. Pailleux, D. Vasiljević, M. Hamrud, A. Hollingsworth, F. Rabier, and M. Fisher, 1998: The ECMWF implementation of three dimensional variational assimilation (3D-Var). Part I: Formulation. *Quart. J. Roy. Meteor. Soc.,* **124**, 1783–1808.

DAO, 1996: Algorithm Theoretical Basis Document Version 1.01, Data Assimilation Office, NASA's Goddard Space Flight Center. Available on-line from

http://dao.gsfc.nasa.gov/subpages/atbd.html

da Silva, A. and J. Guo, 1996: Documentation of the Physical-space Statistical Analysis System (PSAS) Part I: The Conjugate Gradient Solver Version, PSAS-1.00. *DAO Office Note 96-02*, Data Assimilation Office, Goddard Space Flight Center, Greenbelt, MD 20771. Available on-line from

http://dao.gsfc.nasa.gov/subpages/office-notes.html

da Silva, A. and C. Redder, 1995: Documentation of the GEOS/DAS Observation Data Stream (ODS), Version 1.01. *DAO Office Note 95-01*, Data Assimilation Office, Goddard Space Flight Center, Greenbelt, MD 20771. Available on-line from

http://dao.gsfc.nasa.gov/subpages/office-notes.html

da Silva A., M. Tippett, J. Guo, 1999: The PSAS User's Manual. To be published as *DAO Office Note 99-XX*. Data Assimilation Office, Goddard Space Flight Center, Greenbelt, MD 20771. Available on-line from

http://dao.gsfc.nasa.gov/subpages/office-notes.html

Gaspari, G. and S. E. Cohn, 1999: Construction of correlation functions in two and three dimensions, *Quart. J. Roy. Met. Soc.,* **125**, 723–757.

Gaspari, G., S. E. Cohn, D. P. Dee, J. Guo, and A. M. da Silva, 1998: Construction of the PSAS multi-level forecast error covariance models, *DAO Office Note 98-06, in preparation*, Data Assimilation Office, Goddard Space Flight Center, Greenbelt, MD 20771.

Golub, G. H. and C. F. van Loan, 1989: *Matrix Computations,* 2nd Edition, The John Hopkins University Press, 642 pp.

Larson, J., J. Guo, G. Gaspari, A. da Silva, and P. M. Lyster 1998: Documentation of the Physical-space Statistical Analysis System (PSAS) Part III: The Software Implementation. *DAO Office Note 98-05*, Data Assimilation Office, Goddard Space Flight Center, Greenbelt, MD 20771. Available on-line from

http://dao.gsfc.nasa.gov/subpages/office-notes.html

Lyster, P. M., 1999: The Computational Complexity of Atmospheric Data Assimilation. Submitted to *Int. J. Appl. Sci. Comp..* Available on-line from

http://dao.gsfc.nasa.gov/DAO_people/lys/complexity

Parrish, D. F. and J. C. Derber, 1992: The National Meteorological Center's spectral statistical-interpolation analysis system. *Mon. Wea. Rev.,* **120**, 1747–1763.

Pfaendtner, 1996: Notes on the Icosohedral Decomposition in PSAS. *DAO Office Note 96-04,* Data Assimilation Office, Goddard Space Flight Center, Greenbelt, MD 20771.

Pfaendtner, J., S. Bloom, D. Lamich, M. Seablom, M. Sienkiewicz, J. Stobie, and A. da Silva, 1995: Documentation of the Goddard Earth Observing System (GEOS) Data Assimilation System–Version 1. *NASA Tech. Memo. No. 104606,* Vol. **4**, NASA Goddard Space Flight Center, Greenbelt, MD 20771. Available on-line from

http://dao.gsfc.nasa.gov/subpages/tech-reports.html

Rabier, F., A. Mc Nally, E. Andersson, P. Courtier, P. Undén, J. Eyre, A. Hollingsworth, and F. Bouttier, 1998: The ECMWF implementation of three dimensional variational assimilation (3D-Var). Part II: Structure functions. *Quart. J. Roy. Meteor. Soc.,* **124**, 1809–1830.